Available online at www.sciencedirect.com
SCIENCE DIRECT®
Journal of Catalysis 224 (2004) 473–478
JOURNAL OF CATALYSIS
www.elsevier.com/locate/jcat

Research Note

# The reaction route and active site of catalytic decomposition of hydrazine over molybdenum nitride catalyst ☆

Xiaowei Chen, Tao Zhang,* Mingyuan Zheng, Zili Wu, Weicheng Wu, and Can Li *

*State Key Laboratory of Catalysis, Dalian Institute of Chemical Physics, Chinese Academy of Sciences, PO Box 110, Dalian 116023, China*

Received 14 November 2003; revised 10 February 2004; accepted 10 February 2004

**Abstract**

The catalytic properties of the passivated, reduced passivated, and fresh bulk molybdenum nitride for hydrazine decomposition were evaluated in a microreactor. The reaction route of hydrazine decomposition over molybdenum nitride catalysts seems to be the same as that of Ir/$\gamma$-$Al_2O_3$ catalysts. Below 673 K, the hydrazine decomposes into $N_2$ and $NH_3$. Above 673 K, the hydrazine decomposes into $N_2$ and $NH_3$ first, and then the produced $NH_3$ further dissociates into $N_2$ and $H_2$. From the in situ FT-IR spectroscopy, hydrazine is adsorbed and decomposes mainly on the Mo site of the $Mo_2N$/$\gamma$-$Al_2O_3$ catalyst.

*Keywords:* Molybdenum nitride; Hydrazine decomposition; FT-IR spectroscopy; Hydrazine adsorption

## 1. Introduction

Recently, the catalytic performances of transition metal nitride and carbide catalysts for hydrazine decomposition have been studied because of their low cost and platinum-like behavior in catalysis [1–6]. Transition metal nitride and carbide catalysts have the potential to substitute for the traditional noble metal catalyst (20–40 wt% Ir/$Al_2O_3$), which has been widely applied to hydrazine decomposition in space technology since the 1970s [7–10].

In 1997, hydrazine decomposition over molybdenum nitride and tungsten carbide catalysts was reported for the first time [1]. Their catalytic properties were similar to those of the iridium catalyst in a thruster. Three years later, tungsten nitride and niobium nitride catalysts were also studied for hydrazine decomposition reaction. The activity of niobium nitride was lower than that of tungsten nitride and iridium catalysts [2]. Moreover, alumina-supported molybdenum nitride and carbide catalysts are active as Ir catalysts for hydrazine decomposition in the thruster [5,6].

Generally speaking, there are two typical reaction routes for hydrazine decomposition as depicted in Eqs. (1) and (2) [8,9,11]. The produced ammonia decomposes further into nitrogen and hydrogen at elevated temperatures according to Eq. (3). Eq. (4) describes the overall reaction of hydrazine decomposition. In Eq. (4), $X$ is defined as the selectivity of hydrazine decomposition, which is the decomposition percentage of hydrazine followed by Eq. (1):

$$N_2H_4 = N_2 + 2H_2, \tag{1}$$

$$3N_2H_4 = N_2 + 4NH_3, \tag{2}$$

$$2NH_3 = N_2 + 3H_2, \tag{3}$$

$$3N_2H_4 = 4(1-X)NH_3 + (1+2X)N_2 + 6XH_2. \tag{4}$$

It has been reported that the reaction route of hydrazine decomposition depends on the metal and the temperature range [11]. For instance, the main reaction over Ir, Ni, Co, Ru, Ag, and Cu catalysts proceeds through Eq. (2), while reactions (1) and (2) can take place over Rh, Pt, and Pd catalysts at the same time between 333 and 433 K [3]. Furthermore, the products of hydrazine decomposition over tungsten carbide catalysts are nitrogen and ammonia, suggesting that the reaction route is through Eq. (2) [3].

Although the catalytic performances of transition metal nitrides and carbides for hydrazine decomposition have been studied extensively, little attention has been paid to the intrinsic activity, reaction route, and active site on transition

---

☆ This work was supported by a grant from the Natural Science Foundation of China (NSFC) for Outstanding Youth (No. 20325620).

* Corresponding authors.

*E-mail addresses:* taozhang@dicp.ac.cn (T. Zhang), canli@dicp.ac.cn (C. Li).

0021-9517/$ – see front matter © 2004 Elsevier Inc. All rights reserved.
doi:10.1016/j.jcat.2004.02.035

metal nitride and carbide catalysts. In this work, the catalytic activities of passivated, reduced passivated, and fresh molybdenum nitride catalysts for hydrazine decomposition evaluated in a microreactor are compared in order to correlate the catalysis nature and surface chemistry of molybdenum nitride catalysts. FT-IR spectroscopy, combined with the adsorption of probe molecules, has been employed to characterize the surface of molybdenum nitride catalysts [12–14]. The hydrazine adsorption and decomposition over a $Mo_2N/\gamma$-$Al_2O_3$ catalyst were investigated by in situ FT-IR spectroscopy for the first time. The reaction route of hydrazine decomposition over molybdenum nitride catalyst is also proposed.

## 2. Experimental

### 2.1. Catalyst preparation

Bulk molybdenum nitride catalyst was prepared by temperature-programmed reaction of $MoO_3$ and ammonia ($\geqslant$ 99.99%). The temperature was increased from room temperature to 573 K at a rate of 5 K/min and then to 973 K at a rate of 1 K/min, and finally was kept at the terminal temperature for 2 h. The nitrided sample was cooled to room temperature in a flow of ammonia and passivated with a mixture of 1 vol% $O_2/N_2$ to avoid the violent oxidation of the prepared catalyst before exposure to air. The BET specific surface area of the passivated bulk $Mo_2N$ is 104 $m^2/g$. The XRD result shows that the main phase of this sample is $\gamma$-$Mo_2N$.

The supported $Mo_2N/\gamma$-$Al_2O_3$ (8.7 wt%) catalyst was synthesized by nitriding $MoO_3/\gamma$-$Al_2O_3$ precursor with ammonia. The nitrided and passivated procedures are the same as those for the bulk molybdenum nitride sample. The $MoO_3/\gamma$-$Al_2O_3$ precursor was prepared by the incipient wetness method using an aqueous $(NH_4)_6Mo_7O_{24}\cdot 4H_2O$ solution and $\gamma$-$Al_2O_3$, followed by drying at 393 K for 12 h and calcination at 773 K for 4 h. The BET specific surface area of $\gamma$-$Al_2O_3$ is 198 $m^2/g$.

A commercial 31.6 wt% $Ir/Al_2O_3$ catalyst with BET specific area of 164.9 $m^2/g$ was used and compared with the molybdenum nitride catalyst in the catalytic activity test and $NH_3$-TPD experiment. In order to obtain good transmission in IR measurements, $Ir/Al_2O_3$ and $Mo_2N/Al_2O_3$ with lower metal loadings (7.7 and 8.7 wt%, respectively) were used. The 7.7 wt% $Ir/\gamma$-$Al_2O_3$ catalyst was prepared by the incipient wetness method using an aqueous solution of $H_2IrCl_6$ and $\gamma$-$Al_2O_3$ (198 $m^2/g$), and then dried at 393 K for 12 h and calcinated at 673 K for 4 h.

### 2.2. Catalyst tests

The catalytic activities were evaluated in a fixed-bed continuous flow microreactor. The temperature of liquid hydrazine remained at 303 K and a flow of Ar gas was passed through the liquid hydrazine. The feedstock consists of about 3 vol% $N_2H_4$ in Ar. The space velocity of the $N_2H_4$/Ar mixture was 17,000 $h^{-1}$. A 0.04 ml catalyst and 0.26 ml silica were mixed together and placed in the quartz reactor. Different activation procedures were used. Before the reaction test, the fresh $Mo_2N$ was obtained by renitriding the passivated $Mo_2N$ through a flow of ammonia ($\geqslant$ 99.99%). The flow rate of ammonia is 100 ml/min. The temperature was raised to 973 K with a rate of 10 K/min and held at this temperature for 1 h. The passivated $Mo_2N$ catalyst was reduced by $H_2$ at 773 K for 1 h and is called reduced passivated $Mo_2N$ catalyst. The 31.6 wt% $Ir/Al_2O_3$ catalyst was also reduced by $H_2$ at 773 K for 1 h before the catalytic test. The initial reaction temperature was 303 K and was gradually increased until $N_2$ and $H_2$ were detected as the main products of reaction.

The feedstock and the product analysis were carried out using an on-line gas chromatograph (Agilent-6890) equipped with a thermal conductivity detector and an automatic injection valve. The carrier gas is argon. Separation of the products is achieved using a Chromosorb 102 column and a 13 X molecular sieve column before the detector.

### 2.3. $NH_3$-TPD characterization

Catalysts (200 mg) were reduced at 773 K for 1 h and then were flushed for 0.5 h at 773 K with He. When the temperature was decreased to room temperature, $NH_3$ was injected using a syringe until saturation. During the TPD process the desorbed products were monitored by TCD and a mass spectrometer (Omnistar) at the same time. The signals of $m/e = 2$, 14, 15, 16, 17, 18, and 28 were detected simultaneously.

### 2.4. FT-IR studies

All the infrared spectra were collected at room temperature on a Fourier transform spectrometer (Nicolet Impact 410) with a resolution of 4 $cm^{-1}$ and 64 scans in the region 4000–1000 $cm^{-1}$. A passivated 8.7 wt% $Mo_2N/\gamma$-$Al_2O_3$ sample was pressed into a self-supporting wafer and put into a quartz IR cell with $CaF_2$ windows. The passivated sample was heated in ammonia from room temperature to 623 K at a rate of 10 K/min, and then to 723 K at a rate of 1 K/min, further from 723 to 903 K at a rate of 3 K/min, and then held at this temperature for 1 h. The passivated sample renitrided by $NH_3$ in the IR cell is called fresh $Mo_2N/\gamma$-$Al_2O_3$ sample, while the passivated sample treated with $H_2$ at 773 K for 1 h is denoted as reduced passivated $Mo_2N/\gamma$-$Al_2O_3$. Before adsorption the as-prepared sample was held in vacuum at 773 K for 1 h and then cooled to room temperature. All the spectra were obtained at RT after the system was evacuated at $10^{-2}$ Pa.

## 3. Results and discussion

Previous literature shows that the surface of fresh, reduced passivated, and passivated molybdenum nitride catalyst is quite different [12,13]. However, most studies about the catalytic decomposition of hydrazine over passivated transition metal nitrides and carbides were investigated in thrusters on which there is a thin oxynitride or oxycarbide layer on the surface of the catalyst [1,2,4–6]. In order to gain sight into the intrinsic catalytic property of molybdenum nitride catalyst, the catalytic activities of passivated, reduced passivated, and fresh bulk $Mo_2N$ catalysts for hydrazine decomposition versus reaction time at 303 K were compared in the microreactor (Fig. 1). It can be seen that the conversion of hydrazine over the passivated $Mo_2N$ catalyst is only about 20% at the beginning and then decreases slightly with reaction time. The hydrazine conversion declines to 7% after 240 min on stream. After the passivated $Mo_2N$ catalyst was reduced with $H_2$ at 773 K for 1 h, the catalytic activities for hydrazine decomposition increase significantly. The hydrazine conversion is around 90% and then tends to be stable at the level of 80%. It was reported that after the passivated $Mo_2N$ sample was renitrided at 973 K, the BET specific surface area, the crystal structure, and the $H_2$ uptake characteristics are similar to those of the fresh one [12–15]. As seen in Fig. 1, the conversion of hydrazine over a fresh $Mo_2N$ catalyst remains 100% in the initial 20 min on stream, and then decreases slightly with the increase of reaction time. This result indicates that there is no big difference between the fresh and the reduced passivated $Mo_2N$ catalysts. However, the catalytic activities of the passivated $Mo_2N$ catalyst are relatively lower than those of the fresh $Mo_2N$ catalyst. The lower activity of the passivated $Mo_2N$ catalyst is due to the passivated procedure, which leads to great change on the surface of the $Mo_2N$ catalyst.

As noted in Section 1, hydrazine decomposes into hydrogen, nitrogen, and ammonia by two reaction routes. In order to know the reaction route of hydrazine decomposition over molybdenum nitride catalysts, thermal decomposition and catalytic decomposition over the commercial Ir/$\gamma$-$Al_2O_3$ catalyst and fresh bulk $Mo_2N$ catalyst are shown in Fig. 2.

Without any catalyst, no reaction occurs when the reaction temperature is below 473 K. As soon as the reaction temperature is up to 473 K, hydrazine begins to decompose into $N_2$ and $NH_3$. The conversion of hydrazine increases with increasing reaction time. Hydrazine decomposes completely at 513 K. When the reaction temperature is increased gradually, $H_2$ begins to appear and the selectivity to reaction (1) increases. The selectivity to $H_2$ is about 15% at 973 K. For the thermal decomposition of hydrazine, the main reaction is reaction (2) below 873 K.

The hydrazine conversion is 100% over 31.6 wt% Ir/$Al_2$-$O_3$ catalyst even at 303 K. Below 573 K, the main products of hydrazine decomposition are $N_2$ and $NH_3$, and then the selectivity increases with increasing reaction temperature. $N_2$, $H_2$, and $NH_3$ exist in the products of hydrazine decomposition at the same time. When the temperature is up to 723 K, $NH_3$ vanishes, and the selectivity of the catalyst is

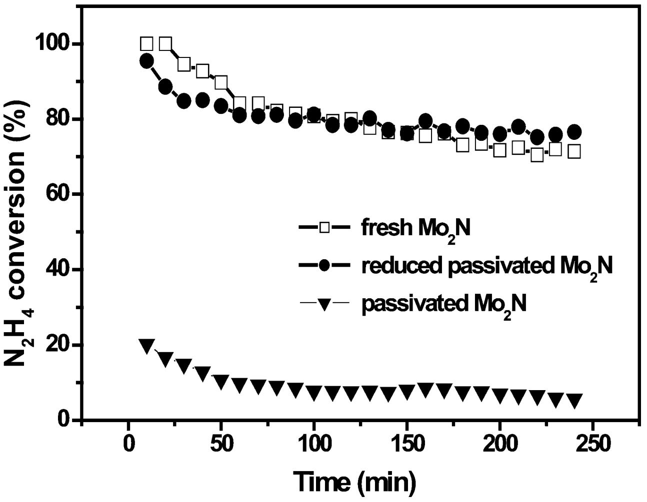

Fig. 1. Hydrazine decomposition over fresh, reduced passivated, and passivated bulk $Mo_2N$ catalysts at 303 K.

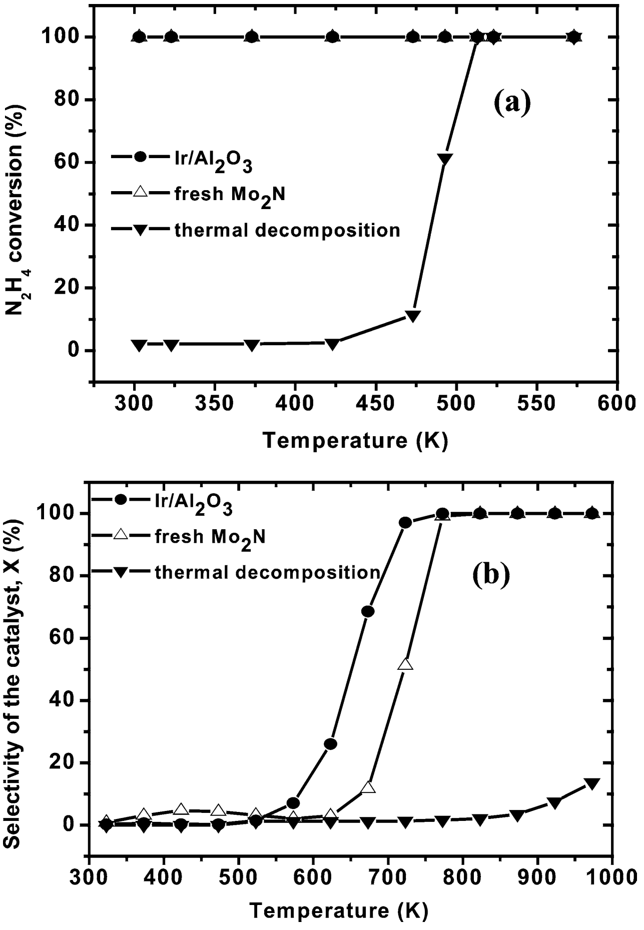

Fig. 2. Thermal decomposition of hydrazine and catalytic decomposition of hydrazine on fresh bulk $Mo_2N$ and 31.6 wt% Ir/$\gamma$-$Al_2O_3$ catalysts: (a) hydrazine conversion, (b) selectivity of hydrazine decomposition.

100%; that is, hydrazine decomposes mainly through reaction (1). Similar to the Ir/$\gamma$-$Al_2O_3$ catalyst, the main products are $N_2$ and $NH_3$ below 673 K over fresh $Mo_2N$ catalyst and then the selectivity of the catalyst begins to increase with increasing reaction temperature. $H_2$ starts to be produced when the temperature is above 773 K and the hydrazine decomposition is mainly followed by reaction route (1).

The produced ammonia could decompose into nitrogen and hydrogen at elevated temperatures. It has been reported that both Ir/$\gamma$-$Al_2O_3$ and transition metal nitrides are excellent catalysts for $NH_3$ decomposition [16–20]. In order to make sure that the produced ammonia decomposes into $N_2$ and $H_2$ at the elevated temperatures, $NH_3$-TPD over $\gamma$-$Al_2O_3$, commercial 31.6 wt% Ir/$Al_2O_3$, and bulk $Mo_2N$ catalysts were studied. As seen in Fig. 3, the maximum $NH_3$ desorption (mass = 16) appears around 370 K on the $\gamma$-$Al_2O_3$ support. No $N_2$ (mass = 28) and $H_2$ (mass = 2) desorption peaks are observed. $NH_3$ desorbs from the Ir/$\gamma$-$Al_2O_3$ catalyst from 330 to 430 K. The desorption of $N_2$ commences in the temperature region of 500–700 K; meanwhile, a $H_2$ desorption peak appears. Therefore, the desorption peaks of $N_2$ and $H_2$ are attributed to $NH_3$ decomposition on Ir/$\gamma$-$Al_2O_3$ catalyst. $NH_3$-TPD for reduced passivated bulk $Mo_2N$ is also shown in Fig. 3. Although there are two kinds of $NH_3$ desorption peaks in the low temperature range (300–600 K), which are different from the Ir/$Al_2O_3$, the desorption of $N_2$ and $H_2$ can also be found in temperatures higher than 600 K. The $N_2$ desorption between 600 and 800 K is accompanied by $H_2$ desorption. It must come from the decomposition of $NH_3$. On the other hand, the $N_2$ desorption peak at temperatures higher than 800 K should be the result of $Mo_2N$ decomposition. The $NH_3$-TPD results suggest that there are active sites for $NH_3$ decomposition on both the Ir/$\gamma$-$Al_2O_3$ and $Mo_2N$ catalysts, and also at elevated temperatures the produced $NH_3$ really decomposes into $N_2$ and $H_2$. The similar product distributions of hydrazine decomposition and similar $NH_3$-TPD profiles over Ir/$\gamma$-$Al_2O_3$ and molybdenum nitride catalysts indicate that hydrazine decomposition experiences similar reaction routes on Ir/$Al_2O_3$ catalysts and fresh $Mo_2N$ catalysts. At lower temperatures, hydrazine decomposes into nitrogen and ammonia. Above 673 K, hydrazine decomposes into nitrogen and ammonia. In the second step the produced ammonia dissociates into nitrogen and hydrogen.

Fig. 4 shows the IR spectra of adsorbed $NH_3$ and $N_2H_4$ on $\gamma$-$Al_2O_3$, $N_2H_4$ on 7.7 wt% Ir/$\gamma$-$Al_2O_3$ catalyst, and gaseous $N_2H_4$. The gas phase of hydrazine has three characteristic IR bands at 3330–3287, 1620, and 1262 $cm^{-1}$ (Fig. 4, a). The 3330–3287 $cm^{-1}$ band can be attributed to the vibrations of N–H stretching, while the bands at 1620 and 1262 $cm^{-1}$ are mainly assigned to the N–H bending vibrations [21]. When $N_2H_4$ is adsorbed on $\gamma$-$Al_2O_3$, the characteristic IR band of $N_2H_4$ is at 1620 $cm^{-1}$. Adsorbed $NH_3$ on $\gamma$-$Al_2O_3$ gives three IR bands at 1620, 1484, and 1260 $cm^{-1}$. These bands are similar to those observed by Contour and Pannetier [9]. IR bands at 1620 and 1260 $cm^{-1}$ could be assigned to the adsorbed $NH_3$ on the Lewis acid site of $\gamma$-$Al_2O_3$, and the band at 1484 $cm^{-1}$ could be attributed to ammonium ions. $N_2H_4$ adsorption on the reduced Ir/$\gamma$-$Al_2O_3$ catalyst at 773 K shows absorbance features at 1620, 1484, and 1262 $cm^{-1}$ (see Fig. 4,d). Considering the results of $NH_3$ and $N_2H_4$ adsorption on $\gamma$-$Al_2O_3$, the band at 1484 $cm^{-1}$ can be attributed to the $NH_4^+$, which is produced by $NH_3$ adsorption on the surface of the catalyst. These results suggest that hydrazine decomposition occurs on the Ir/$\gamma$-$Al_2O_3$ catalyst because the band at 1484 $cm^{-1}$ is not observed when $N_2H_4$ is adsorbed on the surface of $\gamma$-$Al_2O_3$;

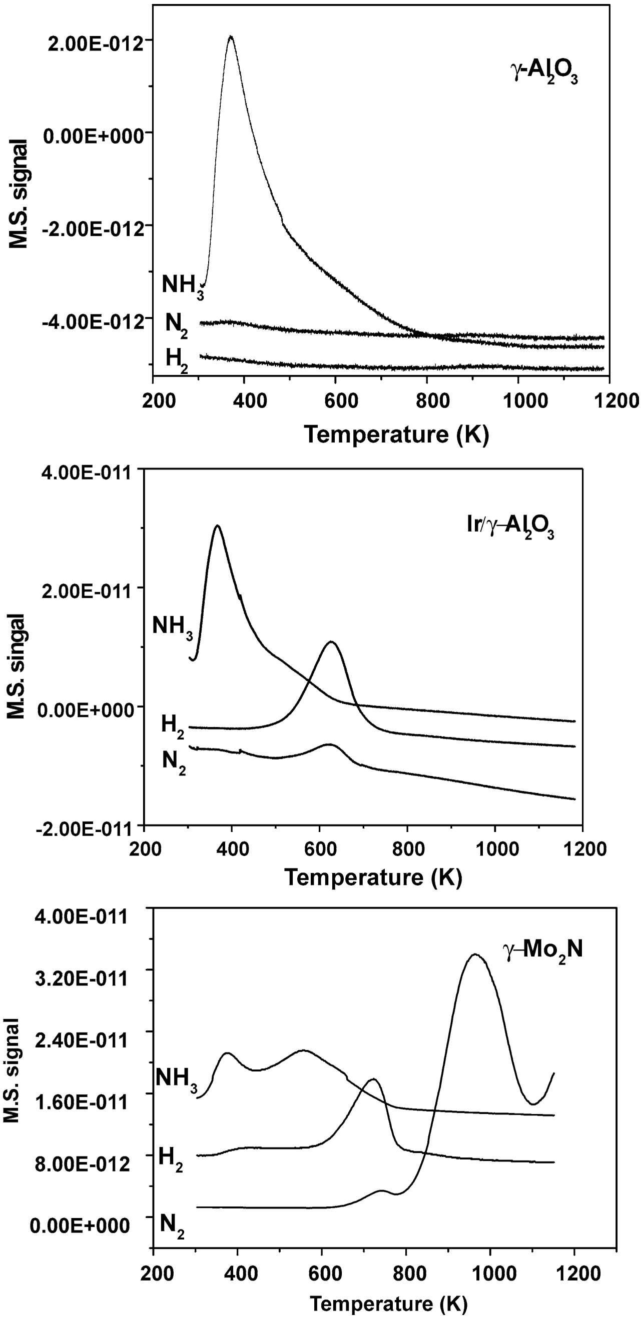

Fig. 3. The $NH_3$-TPD profiles (mass spectroscopy) of $\gamma$-$Al_2O_3$, 31.6 wt% Ir/$\gamma$-$Al_2O_3$, and reduced passivated bulk $Mo_2N$.

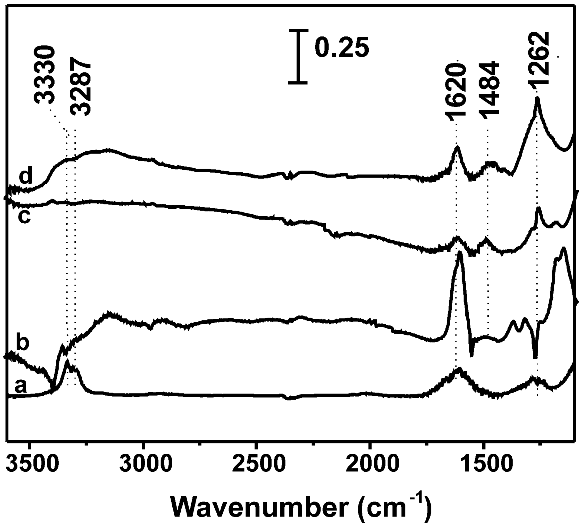

Fig. 4. IR spectra of (a) gaseous $N_2H_4$, (b) $N_2H_4$ adsorbed on $\gamma$-$Al_2O_3$, (c) $NH_3$ adsorbed on $\gamma$-$Al_2O_3$, and (d) $N_2H_4$ adsorbed on 7.7 wt% Ir/$\gamma$-$Al_2O_3$ at RT.

Table 1
Assignment of the IR bands from $NH_3$ and $N_2H_4$ adsorption on $\gamma$-$Al_2O_3$, 7.7 wt% Ir/$\gamma$-$Al_2O_3$, and 8.7 wt% $Mo_2N$/$\gamma$-$Al_2O_3$ catalysts

| Species | Gas phase | $\gamma$-$Al_2O_3$ | Ir/$\gamma$-$Al_2O_3$ | $Mo_2N$/$\gamma$-$Al_2O_3$ | Assignment |
|---|---|---|---|---|---|
| $NH_3$ | 3337–3414 | | | | $\nu$(NH) |
| | 1628 | 1620 | 1620 | 1620 | $\delta$(NH) |
| | | 1484 | 1484 | 1484 | $NH_4^+$ |
| | 950 | 1260 | 1260 | 1260 | $\delta$(NH) |
| $N_2H_4$ | 3330–3287 | 3330–3287 | 3330–3287 | 3330–3287 | $\nu$(NH) |
| | 1620 | 1601 | 1620 | 1620 | $\delta$(NH) |
| | 1262 | | 1260 | 1260 | $\delta$(NH) |
| | | | 1484 | 1484 | $NH_4^+$ |

however, the band at 1484 cm$^{-1}$ is seen when $N_2H_4$ is adsorbed on the Ir/$\gamma$-$Al_2O_3$ catalyst. The assignment of the IR bands from $NH_3$ and $N_2H_4$ adsorption on $\gamma$-$Al_2O_3$ and Ir/$\gamma$-$Al_2O_3$ catalysts is listed in Table 1.

As described before, the fresh and reduced passivated $Mo_2N$/$\gamma$-$Al_2O_3$ catalysts have a much higher activity than the passivated $Mo_2N$/$\gamma$-$Al_2O_3$ catalyst. $N_2H_4$ adsorptions on passivated, reduced passivated, and fresh $Mo_2N$/$\gamma$-$Al_2O_3$ catalysts were therefore studied using in situ IR spectra (shown in Fig. 5). $N_2H_4$ adsorption on passivated $Mo_2N$/$\gamma$-$Al_2O_3$ catalyst gives IR bands at 3330–3287, 1620, and 1455 cm$^{-1}$. However, the characteristic IR bands of $N_2H_4$ adsorption on reduced passivated and fresh $Mo_2N$/$\gamma$-$Al_2O_3$ catalysts appear at 3330, 1620, and 1484 cm$^{-1}$, similar to the adsorption of $N_2H_4$ on Ir/$\gamma$-$Al_2O_3$ catalysts. The band of $NH_3$ adsorption on the Brønsted acid site of fresh and reduced passivated $Mo_2N$/$\gamma$-$Al_2O_3$ catalysts (1484 cm$^{-1}$) shifts to lower frequencies (1455 cm$^{-1}$) when hydrazine is adsorbed on the passivated $Mo_2N$/$\gamma$-$Al_2O_3$ catalyst. This result is possibly due to the oxynitride layer on the surface of passivated catalyst [22]. The oxygen atom on the surface of passivated $Mo_2N$/$\gamma$-$Al_2O_3$ catalyst has a significant effect on the adsorption and reaction properties of fresh $Mo_2N$/$\gamma$-$Al_2O_3$ catalyst for hydrazine decomposition. Yang et al. found that the surface of reduced passivated $Mo_2N$/$\gamma$-$Al_2O_3$ catalyst is in a highly oxidic form; i.e., most Mo sites are in high valence state (+4). When the sample is renitrided at a temperature as high as 873 K, the surface molybdenum atoms can be reduced to $Mo^{\delta+}$ ($0 < \delta < 2$) cations [12]. These similar catalytic results are probably because there is no obvious difference of hydrazine adsorption and reaction behaviors. These suggest that when the valence state of Mo atom on the surface of $Mo_2N$/$\gamma$-$Al_2O_3$ catalysts is lower than or equal to +4, the $Mo_2N$/$\gamma$-$Al_2O_3$ catalysts have catalytic activities close to those of Ir/$\gamma$-$Al_2O_3$ catalysts for hydrazine decomposition.

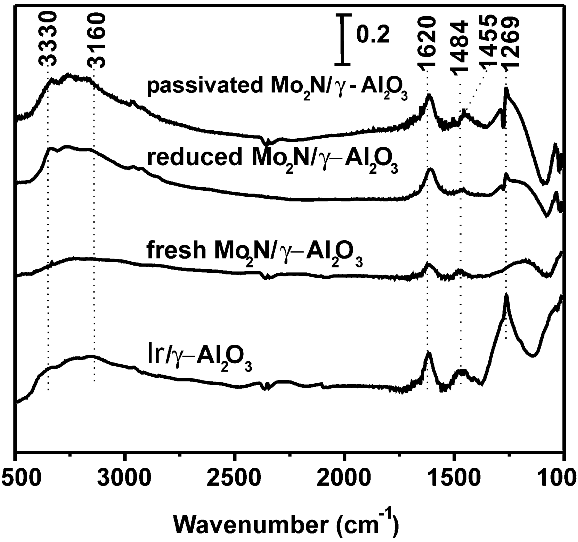

Fig. 5. IR spectra of $N_2H_4$ adsorption on 7.7 wt% Ir/$\gamma$-$Al_2O_3$ catalysts and 8.7 wt% $Mo_2N$/$\gamma$-$Al_2O_3$ catalysts with different states.

As seen in Fig. 6, CO adsorption on the fresh $Mo_2N$/$\gamma$-$Al_2O_3$ catalyst gives two characteristic IR bands at 2045 and 2200 cm$^{-1}$, corresponding to the adsorbed CO on the surface Mo and N sites, respectively, forming linearly adsorbed CO and NCO species [12]. When $N_2H_4$ is adsorbed on the CO-preadsorbed $Mo_2N$/$\gamma$-$Al_2O_3$ catalyst, the band at 2200 shifts to 2191 cm$^{-1}$, while the band at 2045 cm$^{-1}$ disappears, accompanied by the appearance of a new band at 2240 cm$^{-1}$. This band may be assigned to one or several of the following possible species:

(1) NCO species,
(2) Mo–NC (or Mo–CN) species,
(3) Al–NC (or Al-CN) species, or
(4) Al–NCO species [13].

At the same time, the bands at 1620 and 1484 cm$^{-1}$ were seen which can be attributed to $N_2H_4$ adsorption and reaction on the $Mo_2N$/$\gamma$-$Al_2O_3$ catalyst. The disappearance of the band at 2045 cm$^{-1}$, which is assigned to the adsorbed CO on the Mo site of the $Mo_2N$/$\gamma$-$Al_2O_3$ catalyst, suggests that $N_2H_4$ is adsorbed mainly on the Mo site and then de-

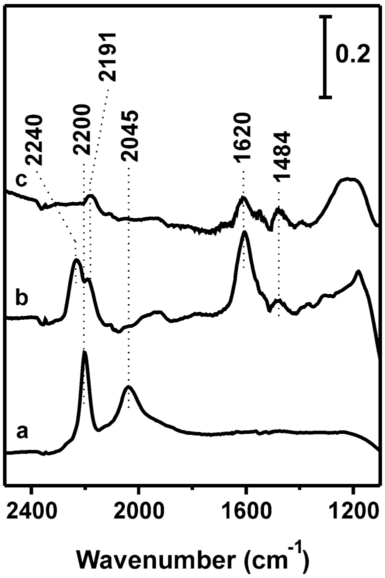

Fig. 6. IR spectra of CO and $N_2H_4$ coadsorbed on fresh 8.7 wt% $Mo_2N/\gamma\text{-}Al_2O_3$ catalyst at RT: (a) CO alone, (b) CO preadsorbed, then $N_2H_4$, (c) $N_2H_4$ preadsorbed, then CO.

composes to $NH_3$ and $N_2$ over it. When $N_2H_4$ is preadsorbed on the $Mo_2N/\gamma\text{-}Al_2O_3$ catalyst, subsequently adsorbed CO gives one band at 2191 $cm^{-1}$ and the band at 2045 $cm^{-1}$ does not appear. This reveals that $N_2H_4$ adsorption on the $Mo_2N/\gamma\text{-}Al_2O_3$ catalyst is so strong that it covers the adsorption site of the catalyst, so the IR band of CO adsorption on the Mo sites is not observed. These results show that hydrazine is mainly adsorbed and decomposes on the Mo site of the $Mo_2N/\gamma\text{-}Al_2O_3$ catalyst.

## 4. Conclusions

The performances of molybdenum nitride catalysts with different states for hydrazine decomposition have been studied in the microreactor. The catalytic activity for hydrazine decomposition over passivated molybdenum nitride is much lower than those of reduced passivated and fresh molybdenum nitride catalysts. The reaction route of hydrazine decomposition over a molybdenum nitride catalyst is similar to that of a $Ir/\gamma\text{-}Al_2O_3$ catalyst. Below 673 K, hydrazine mainly decomposes into $N_2$ and $NH_3$; when the reaction temperature is up to 673 K, hydrazine decomposes into $N_2$ and $NH_3$ at first, and then the produced $NH_3$ begins to dissociate into $N_2$ and $H_2$.

The hydrazine adsorption and reaction behaviors over $Mo_2N/\gamma\text{-}Al_2O_3$ catalysts were investigated by in situ FT-IR spectroscopy for the first time. It is found that IR spectra of adsorbed hydrazine over the reduced passivated and fresh $Mo_2N/\gamma-Al_2O_3$ catalysts are also similar to those of $Ir/\gamma\text{-}Al_2O_3$ catalysts. This provides new evidence for the similarities of molybdenum nitride with platinum metal in catalysis. With assistance of the IR technique, $N_2H_4$ adsorption tests on the nitride surface, containing preadsorbed CO, suggest that the adsorption occurs mainly on the Mo site of $Mo_2N/\gamma\text{-}Al_2O_3$ catalysts.

## References

[1] J.A.J. Rodrigues, G.M. Cruz, G. Bugli, M. Boudart, G. Djéga-Mariadassou, Catal. Lett. 45 (1997) 1.
[2] R. Brayner, G. Djéga-Mariadassou, G.M. Cruz, J.A.J. Rodrigues, Catal. Today 57 (2000) 225.
[3] J.B.O. Santos, G.P. Valença, J.A.J. Rodrigues, J. Catal. 210 (2002) 1.
[4] J.A.J. Rodrigues, G.M. Cruz, G. Djéga-Mariadassou, J.N. Hinckel, PCT Int. Appl., WO 96/33803, 1996.
[5] X. Chen, T. Zhang, L. Xia, T. Li, M. Zheng, Z. Wu, X. Wang, Z. Wei, Q. Xin, C. Li, Catal. Lett. 79 (2002) 21.
[6] X. Chen, T. Zhang, P. Ying, M. Zheng, W. Wu, L. Xia, T. Li, X. Wang, C. Li, Chem. Commun. (2002) 288.
[7] W.E. Armstrong, L.B. Ryland, H.H. Voge, US patent 4 124 538, 1978.
[8] W. Keim, in: G. Ertl, H. Knözinger, J. Weitkamp (Eds.), Handbook of Heterogeneous Catalysis, VCH, Weinheim, 1997, p. 1795.
[9] J.P. Contour, G. Pannetier, J. Catal. 24 (1972) 434.
[10] B.J. Wood, H. Wise, J. Catal. 39 (1975) 471.
[11] R. Maurel, J.C. Menezo, J. Catal. 51 (1978) 293.
[12] S. Yang, C. Li, J. Xu, Q. Xin, Chem. Commun. (1997) 1247.
[13] Z. Wu, Y. Chu, S. Yang, Z. Wei, C. Li, Q. Xin, J. Catal. 194 (2000) 23.
[14] Z. Wu, C. Li, Z. Wei, P. Ying, Q. Xin, J. Phys. Chem. B 106 (2002) 979.
[15] G.W. Haddix, J.A. Reimer, A.T. Bell, J. Catal. 108 (1987) 50.
[16] S. Mary, C. Kappenstein, S. Balcon, S. Rossignol, E. Gengembre, Appl. Catal. A 182 (1999) 317.
[17] S. Balcon, C. Kappenstein, S. Mary, E. Gengembre, Appl. Catal. A 196 (2000) 179.
[18] C. Liang, W. Li, Q. Xin, C. Li, Ind. Eng. Chem. Res. 39 (2000) 3964.
[19] S.T. Oyama, Catal. Today 15 (1992) 179.
[20] S.T. Oyama, J. Catal. 133 (1992) 358.
[21] P.A. Giguère, I.D. Liu, J. Chem. Phys. 20 (1952) 136.
[22] M. Nagai, Y. Goto, A. Irisawa, S. Omi, J. Catal. 191 (2000) 128.